Sensors and Materials, Vol. 37, No. 3 (2025) 901–909
MYU Tokyo

S & M 3964

Effects of Electrode Structures on the Sensing Characteristics of Capacitive Accelerometers

Ho Sheng Chen,[1] Rui-Zhi Shi,[2] Kao-Wei Min,[3]
Shao-Jun Luo,[2] Cheng-Fu Yang,[2,4*] and Yan-Zuo Chang[5**]

[1]College of Mechanical and Electrical Engineering, Guangdong University of Petrochemical Technology, Maoming, Guangdong Province 525000, China
[2]Department of Chemical and Materials Engineering, National University of Kaohsiung, Kaohsiung 811, Taiwan
[3]Department of Electronic Engineering, Lunghwa University of Science and Technology, Taoyuan City 333, Taiwan
[4]Department of Aeronautical Engineering, Chaoyang University of Technology, Taichung 413, Taiwan
[5]School of Energy and Power Engineering, Guangdong University of Petrochemical Technology, Maoming, Guangdong Province 525000, China

(Received January 27, 2025; accepted February 21, 2025)

Keywords: electrode structure, sensing characteristics, capacitive accelerometer, COMSOL multiphysics

In this study, COMSOL Multiphysics® (version 6.0) finite element software was used to simulate a sophisticated single-axis accelerometer with different electrode pairs. The first variable in the simulation was the number of electrode pairs in the original accelerometer, which ranged from one to 21, while keeping the mass block length constant. The second variable involved reducing the number of electrode pairs while simultaneously shortening the mass block length. The acceleration levels used in the simulation were 25, 50, and 75*g*, with no changes made to the thickness of the spring element or the external fixed and movable comb electrodes. In our analysis, we focused on evaluating the impact of these parameter variations on several key indicators: the induced displacement, voltage, and maximum von Mises stress within the accelerometer structure. By systematically varying the acceleration level and electrode configuration of the accelerometer, we aimed to understand how these changes affected the performance characteristics of the designed devices. This approach enables us to gain deeper insights into the structural behavior of the accelerometer under different operating conditions, providing valuable data for optimizing its design and functionality in practical applications.

1. Introduction

With technological advancements, the scope of "manufacturing" is no longer limited to automated production. Sensors have become indispensable in modern manufacturing, whether it is for detecting equipment abnormalities, predicting component lifespans, or integrating machine tool networks. For example, to identify the cause of abnormal vibrations during the machining process, accelerometers are used to measure and analyze vibration signals. Similarly, to understand how temperature changes affect thermal deformation in machine tools, data from

*Corresponding author: e-mail: cfyang@nuk.edu.tw
**Corresponding author: e-mail: 1936532762@qq.com
https://doi.org/10.18494/SAM5575

ISSN 0914-4935
https://myukk.org/

displacement and temperature sensors are crucial for building thermal displacement error models.[1] Accelerometers are not only used in factories but are also found in many products we encounter in daily life. In smartphones and tablets, accelerometers are used to detect the device's orientation and to adjust the screen accordingly. For example, when we make a phone call, the phone is typically held vertically, whereas when playing games or watching videos, we usually turn the phone horizontally. The accelerometer detects the phone's direction and tilt, automatically rotating the screen accordingly.[2] In car safety systems, accelerometers are used to trigger airbags during a collision. When a car crashes, the accelerometer quickly senses the impact force and activates the airbags, reducing the risk of injury to the driver.[3]

Additionally, accelerometers help control vehicle stability by monitoring acceleration, assisting the vehicle in maintaining stability during turns or when skidding.[4] In recent years, with the rise of fitness culture, the demand for compact and lightweight devices capable of tracking physical data without interfering with activity has surged. This has led to the rapid development of wearable devices. Today, a smartwatch offers not only calling and alarm features but also utilizes its built-in accelerometer to monitor heart rate, blood pressure, step count, running speed, and more.[5,6] Some high-end models, such as the Galaxy Watch 6, even include fall detection and sleep apnea monitoring. In entertainment, accelerometers are used in motion-based games such as the Wii and Ring Fit, where they detect the movement of game controllers, allowing players to interact with the game through controller movements.[7] Additionally, popular virtual reality (VR) devices now combine accelerometers with gyroscopes for head motion tracking, enhancing the immersive experience in VR and augmented reality (AR) environments.[8] Indeed, accelerometers are highly practical and versatile sensors, effectively meeting the needs across these diverse fields.

The accelerometer structure investigated in this study is a capacitive single-axis accelerometer. The original design consists of fixed electrodes, anchors, folded springs, a mass block, and movable electrodes. When acceleration is applied to the structure, the mass block experiences an inertial force in the opposite direction, causing displacement in the comb-like structure. This displacement results in a change in gap between the two movable electrodes and the fixed electrode, which in turn causes a variation in capacitance between these electrodes. By sensing this capacitance change, we can calculate the acceleration value.[9,10] In this study, two primary design considerations were explored to find the sensing characteristics of a capacitive single-axis accelerometer. The first consideration involved the reduction in the number of sensing electrode pairs from the original 21 pairs to as few as one pair, while keeping the electrode thickness and mass block size unchanged. Reducing the number of electrode pairs makes each pair's contribution more pronounced, as the capacitive changes between pairs of electrodes will have a more significant effect on the overall system's response. As the number of electrode pairs decreases, the system's overall sensitivity increases because the response of each pair to changes in capacitance becomes more significant.

However, such a design comes at the cost of a decrease in resolution. Specifically, when the number of electrode pairs is reduced, although the sensitivity of each pair increases, the granularity of the signal across the measurement range becomes coarser, potentially reducing the precision in some cases. Furthermore, reducing the number of electrode pairs diminishes the

system's ability to resist noise. Multiple electrode pairs can spread out external or internal interference, reducing the noise impact on each pair; however, fewer electrode pairs make the system more sensitive to noise. Despite this, reducing the number of electrode pairs may simplify the manufacturing process, potentially lowering costs, but it will also place higher demands on the precision of the manufacturing process. The second consideration is the effect of reducing the number of electrode pairs while keeping the electrode thickness unchanged, but also shrinking the mass block. The mass block plays a crucial role in sensing acceleration changes on the basis of its mass and inertia. Shrinking the mass block directly impacts the accelerometer's sensitivity and measurement range. A smaller mass block means reduced inertia, causing the displacement of the mass block to be smaller under the same level of acceleration, thereby reducing the amplitude of capacitance change. This results in a decrease in sensitivity.

Specifically, the system may become more sensitive to smaller accelerations but lose its ability to measure larger accelerations. Additionally, a smaller mass block reduces the system's resistance to external interference. A smaller mass block is more sensitive to external vibrations, temperature changes, and other environmental factors, which can affect the accuracy of measurements. Moreover, a smaller mass block may enhance the accelerometer's high-frequency response, as the system's mass and spring constant are reduced, leading to faster response. However, this may reduce the sensitivity for low-frequency measurements. Therefore, while a smaller mass block improves high-frequency response, it sacrifices performance in the low-frequency range. Both design modifications offer distinct advantages and challenges. The first design, which reduces the number of electrode pairs, increases sensitivity but also decreases stability and resolution while reducing the system's noise resistance. The second design, which involves reducing the mass block size, enhances high-frequency response but reduces the system's ability to measure a broad range of accelerations and increases sensitivity to external interference. When selecting between these design modifications, it is essential to balance sensitivity, measurement range, stability, and noise immunity on the basis of the specific application requirements. In this study, we used COMSOL (version 6.0) as a simulation tool to modify the structure of the sensing electrode pairs and investigate how these structural parameter changes affect the sensing characteristics.

2. Simulation Parameters

The ADXL150 served as an ideal prototype for this investigation owing to its established reliability in measuring linear acceleration through capacitive sensing technology. In this study, we employed the ADXL150 as the reference accelerometer, a sophisticated single-axis accelerometer that operates on differential capacitive bridge principles. We explored the impact of changes to the electrode structure of the accelerometer on its performance characteristics. The focus was primarily on the effects of varying the number of electrode pairs on the sensor voltage (mV), displacement (μm), and von Mises stress (10^6 N/m^2). These modifications can affect various aspects of the device, including its sensitivity, response time, and overall performance. Investigating the effects of these structural changes is crucial for optimizing the design to enhance the functionality and reliability of the accelerometer. In this investigation, we

established a fundamental electrode configuration where one set consists of two fixed electrodes paired with one sensing electrode. The original accelerometer design incorporated 21 electrode pairs, and our initial investigation focused on varying the number of electrode pairs from one to 21, as depicted in Fig. 1 and denoted as case one.

During the electrode reduction, we maintained equal distances between the sensing electrode and the fixed electrodes on both sides, as indicated by the red double-headed arrows in Fig. 1. Following the initial data analysis, we expanded our investigation to include mass block length as an additional parameter. This extension was motivated by the current industry trend toward device miniaturization. As shown in Figs. 1(a) and 1(b) for case one, reducing the number of electrode pairs creates additional space on the mass block. Therefore, we investigated the impact of simultaneously reducing both the number of electrode pairs and the mass block length on sensing performance. The mass block length was varied from 148 to 448 μm, as illustrated in Figs. 1(c) and 1(b) for case two. During this process, we systematically reduced both the number of electrode pairs and the mass block length according to the specifications outlined in Table 1. Throughout these modifications, we maintained a consistent 24 μm distance between the electrodes and the sensing electrode on both sides. This comprehensive approach allowed us to evaluate how the combined reduction in the number of electrode pairs and the mass block length affects the accelerometer's sensing capabilities while maintaining precise geometric relationships between critical components. Figure 2 shows the complete grid we constructed, which contained a total of 39543 finite elements. The maximum element size was 44.2 μm, the minimum element size was 5.52 μm, the curvature factor was 0.5, the resolution of narrow regions was 0.6, the

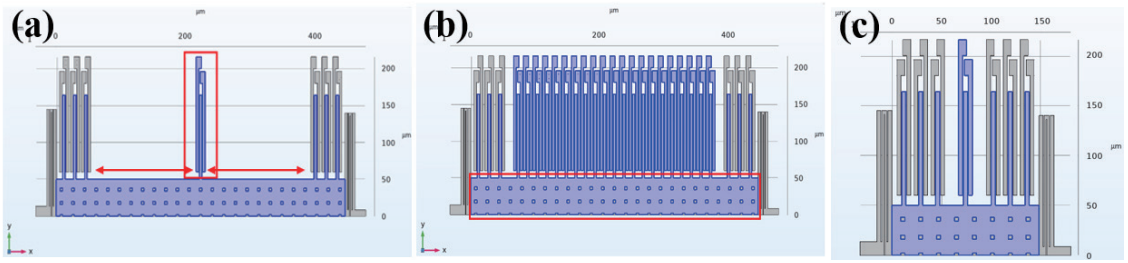

Fig. 1. (Color online) Electrode number variation diagram: (a) one set of electrode pairs, (b) 21 sets of electrode pairs, and (c) one set of electrode pairs with a change in the length of the mass block.

Table 1
Sensor voltages for cases one and two (unit: mV).

No. of electrode pairs	Sensing voltage at 25*g*		Sensing voltage at 50*g*		Sensing voltage at 75*g*	
	Case one	Case two	Case one	Case two	Case one	Case two
1	1.712	2.768	3.431	5.655	5.158	8.544
5	7.659	6.535	15.285	12.915	22.951	19.306
9	12.586	11.117	25.169	22.149	37.821	33.209
13	16.937	15.576	33.862	31.134	50.886	46.749
17	20.857	20.048	41.724	40.081	62.722	60.215
21	24.506	24.506	49.017	49.017	73.692	73.692

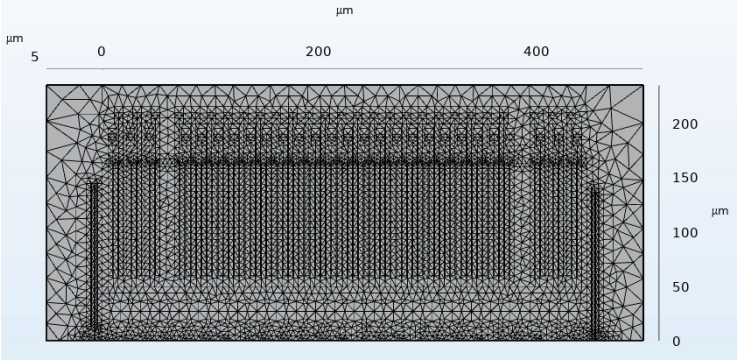

Fig. 2. (Color online) Accelerometer grid diagram.

minimum element quality was 0.1518, the average element quality was 0.5529, and the element volume ratio was 2.413×10^{-3}.

3. Workshop Production Planning Simulation Modeling

As illustrated in Fig. 3(a) for case one, when subjected to 25*g* acceleration, increasing the number of electrode pairs from one to 21 resulted in a voltage rise from 1.712 to 24.506 mV. At 50*g* acceleration, the same increase in the number of electrode pairs yielded a larger voltage change, rising from 3.431 to 49.017 mV. At 75*g* acceleration, the voltage increase was even more pronounced, expanding from 5.1581 to 73.692 mV with the same electrode pair configuration change. The sensing voltage demonstrates significant increases corresponding to changes in the number of electrode pairs under various acceleration conditions. Figure 3(b) reveals the combined effects of varying both the number of electrode pairs and the mass block length. At 25*g* acceleration, the sensing voltage increased from 2.768 to 24.506 mV when adjusting from one to 21 electrode pairs while simultaneously modifying the mass block length. This trend continued at higher levels of acceleration, with 50*g* showing an increase from 5.655 to 49.017 mV and 75*g* exhibiting a voltage rise from 8.544 to 73.692 mV. These results demonstrate that the combination of increased number of electrode pairs and mass block length modifications enhances the overall voltage response of the system across different acceleration levels. This section of the results highlights several important observations. First, increasing the number of electrode pairs leads to a higher sensing voltage. This is because adding more electrode pairs within the same mass block area affects the detection range of the sensing voltage. Second, as the number of electrode pairs increases, the sensing voltage range of the accelerometer also broadens.

Conversely, reducing the number of electrode pairs narrows the sensing voltage range. Moreover, compared with changing the electrode thickness, altering the number of electrode pairs reduces the sensing voltage to a smaller range, thereby enhancing the accelerometer's sensitivity. This allows for a more precise detection and measurement of acceleration changes. In applications where detecting very small voltage changes is critical, adjusting the number of

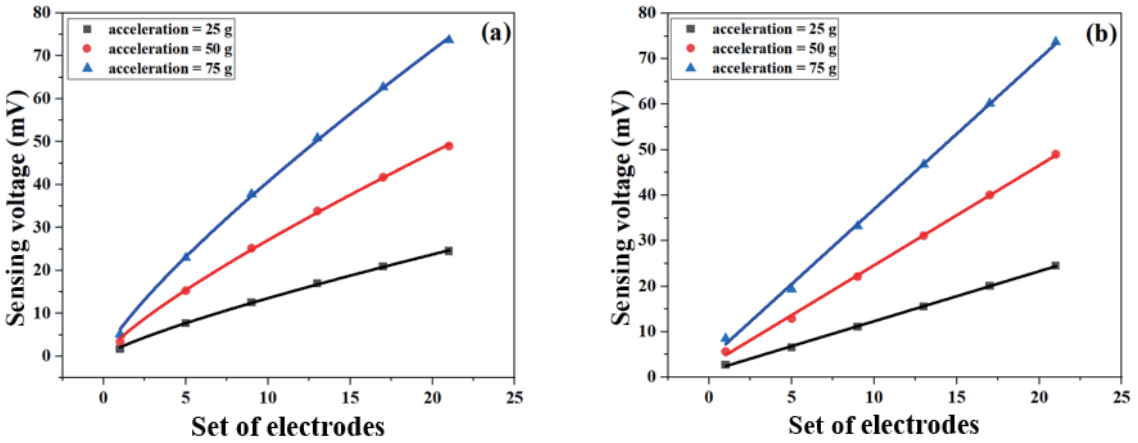

Fig. 3. (Color online) Variation in sensing voltage with the number of electrode pairs at different levels of acceleration: (a) changing the number of electrode pairs and (b) simultaneously changing the number of electrode pairs and mass block length.

electrode pairs becomes an important structural parameter. Third, when we introduced the mass block length parameter, an interesting phenomenon was observed. Generally, when reducing the number of electrode pairs while simultaneously shortening the mass block (case two), the sensing voltage decreases more significantly than when changing only the number of electrode pairs (case one). However, when only one electrode set remains, the sensing voltage response is the opposite. This trend holds for acceleration values of 25, 50, and 75*g*. Initially, we hypothesized that the reduction in mass block size might cause interference between the central sensing electrode and the adjacent self-measuring electrodes. However, from the postprocessing potential and electric field diagrams, it appears that when both the number of electrode pairs and the mass block length are altered, the resulting data shows a lower sensing voltage than when changing only the number of electrode pairs, as illustrated in Fig. 4. Thus, we conclude that there is no interference from the mass block length change.

As shown in Fig. 5(a), increasing the number of electrode pairs results in a linear increase in displacement under three different acceleration conditions. When the number of electrode pairs increases from one to 21, the displacement values at 25, 50, and 75*g* accelerations increase from 0.0253, 0.0507, and 0.076 μm to 0.0341, 0.0682, and 0.1023 μm, respectively. As depicted in Fig. 5(b), when both the number of electrode pairs and the mass block length are increased simultaneously, the displacement increases more notably. For the same increase in the number of electrode pairs from one to 21, the displacement values at 25, 50, and 75*g* accelerations rise from 0.0116, 0.0232, and 0.0347 μm to 0.0341, 0.0682, and 0.1023 μm, respectively. As the number of electrode pairs increases, the range of displacement variation also expands, resulting in an increase in displacement measurement data. In other words, increasing the number of electrode pairs enhances the displacement of the mass block. Additionally, as the level of acceleration increases, the force applied to the mass block also increases, leading to a higher displacement. This trend is more clearly observed in Fig. 5(b), where the length of the mass block is also altered. In this case, the magnitude of displacement increase is more significant than in the case where only the number of electrode pairs is modified. Therefore, when designing accelerometers,

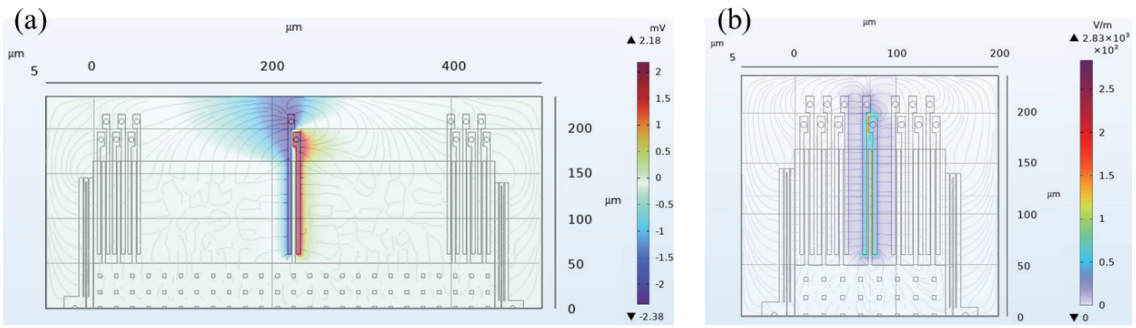

Fig. 4. (Color online) Accelerometer electric field diagram: (a) changing the number of electrode pairs and (b) changing the number of electrode pairs and mass block length.

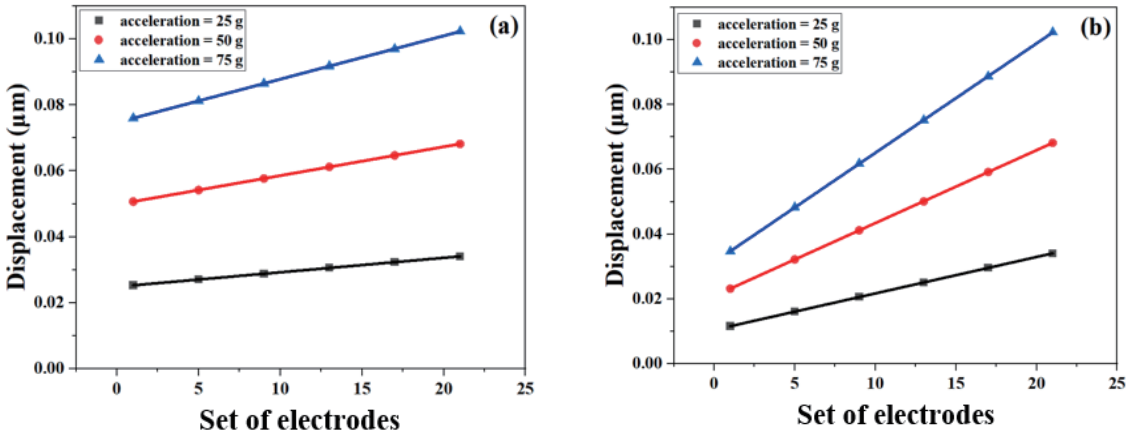

Fig. 5. (Color online) Displacement variation with the number of electrode pairs at different levels of acceleration: (a) changing the number of electrode pairs and (b) changing the number of electrode pairs and mass block length.

if controlling the range of displacement is a priority, adjusting the dimensions of the mass block should be considered as a key factor. This observation highlights the importance of both electrode pair configuration and mass block geometry in controlling the performance of an accelerometer. By adjusting the number of electrode pairs or the dimensions of the mass block, one can optimize the sensitivity and range of the accelerometer to meet specific measurement requirements. Furthermore, the relationship between the level of acceleration and the force applied to the mass block emphasizes how design choices directly affect displacement behavior, which is crucial for precise acceleration measurement.

Finally, we will discuss the variation in von Mises stress with different structural configurations. As shown in Fig. 6(a), under three different acceleration conditions, increasing the number of electrode pairs results in a linear increase in maximum stress. At 25, 50, and 75*g* accelerations, the maximum stress increases from 0.5807, 1.161, and 1.742 × 10^6 N/m^2 to 0.7795, 1.559, and 2.338 × 10^6 N/m^2, respectively. As shown in Fig. 6(b), when both the number of electrode pairs and the mass block length are increased simultaneously, the maximum stress

increases more significantly. At 25, 50, and 75*g* accelerations, the maximum stress increases from 0.2642, 0.5285, and 0.7927 × 10^6 N/m^2 to 0.7795, 1.559, and 2.338 × 10^6 N/m^2, respectively. As the number of electrode pairs increases, the weight of the accelerometer also increases, as shown in Table 2. Consequently, the maximum stress also increases. Additionally, as the level of acceleration increases, the force applied to the mass block also increases, leading to a higher maximum stress. From Fig. 6(b), we can verify this trend. Since the length of the mass block is also altered, the weight of the accelerometer varies significantly, as shown in Table 2. In this case, the increase in maximum stress is more pronounced than in the case where only the number of electrode pairs is changed.

We also observe that changing the dimensions of the mass block not only helps reduce the maximum stress but also has a smaller effect on the sensor voltage, with a relatively minor decrease. Therefore, when designing an accelerometer, adjusting the length of the mass block should be considered as a viable factor. This approach can not only enhance the durability of the accelerometer but also provide a means to control the range of the sensor voltage. The results emphasize the interplay between the design choices, such as the number of electrode pairs and the dimensions of the mass block, and their impact on the accelerometer's performance. Increasing the mass block size appears to mitigate stress concentration and provide a more stable

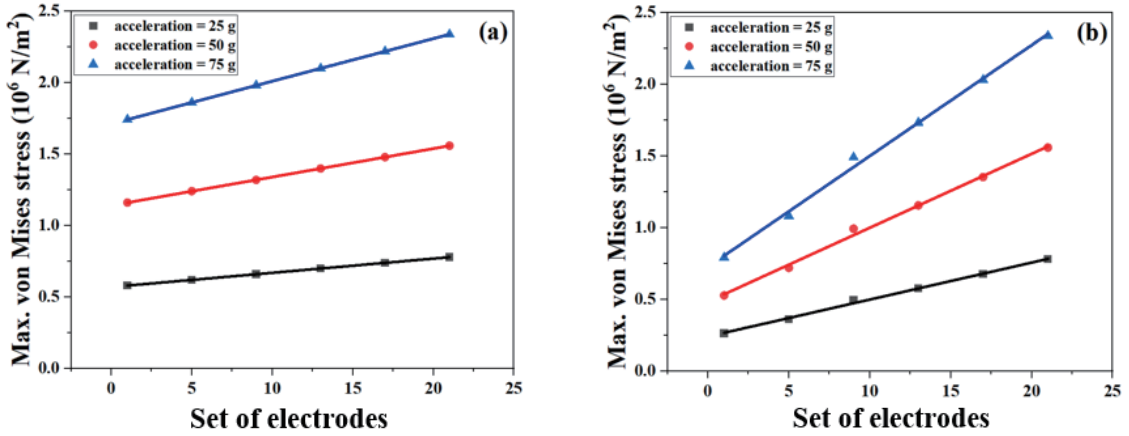

Fig. 6. (Color online) Von Mises stress variation with the number of electrode pairs at different level of acceleration: (a) changing the number of electrode pairs and (b) changing the number of electrode pairs and mass block length.

Table 2
Volume and weight of the accelerometer with different numbers of electrode pairs (case one) and with different numbers of electrode pairs and mass block lengths (case two).

Electrode pairs	Case one		Case two	
	Volume (μm^3)	Weight (10^{-7} g)	Volume (μm^3)	Weight (10^{-7} g)
1	78250	1.815	48250	1.119
5	92627	2.149	68627	1.592
9	10700	2.482	89004	2.065
13	121380	2.816	109380	2.538
17	135760	3.150	129760	3.010
21	150130	3.483	150130	3.483

performance at various levels of accelerations, thus improving durability. Moreover, the minimal impact on sensor voltage changes indicates that such modifications offer a balanced solution for controlling the accelerometer's sensitivity while maintaining its structural integrity. This finding can guide future designs to optimize both the performance and lifespan of accelerometers.

4. Conclusions

In this study, increasing the number of electrode pairs led to a higher sensing voltage, and as the number of electrode pairs increased, the sensing voltage range of the accelerometer also broadened. It was clear that in case two, with fewer electrodes, the sensing voltage was higher than that in case one. When the number of electrode pairs increased from one to 21, it was clear that both the displacement and von Mises stress changes in case two were significantly larger than those in case one. By adjusting the electrode configuration, we could fine-tune the accelerometer's response to acceleration, offering improved sensitivity and performance under different operational conditions. Understanding the relationship between the number of electrode pairs and key metrics such as sensor voltage, displacement, and stress was essential for refining the accelerometer design. This research helped identify optimal configurations that balance sensitivity with durability, ensuring that the accelerometer was both responsive and reliable for a wide range of applications.

Acknowledgments

This research was supported by "Guangdong Science and Technology Program", "Research on Investigation of the Multimodal Intelligent Flying Electric Motorcycle's Autonomous Motion. (NO. 2024A0505050019)", Summit-Tech Resource Corp., and by projects under Nos. NSTC 113-2622-E-390-001 and NSTC 113-2221-E-390-011. We would be like to thank Pitotech Co., Ltd. for their help in teaching the use of COMSOL Multiphysics® software.

References

1 W. Babatain, S. Bhattacharjee, A. M. Hussain, and M. M. Hussain: ACS Appl. Electron. Mater. **3** (2021) 504.
2 Z. Ba, T. Zheng, X. Zhang, Z. Qin, B. Li, X. Liu, and K. Ren: Network and Distributed Systems Security (NDSS) Symposium **2020** (2020) 23–26.
3 L. Zimmermann, J. Ph. Ebersohl, F. Le Hung, J. P. Berry, F. Baillieu, P. Rey, B. Diem, S. Renard, and P. Caillat: Sens. Actuators, A **46** (1995) 190.
4 S. Rafatnia and M. Mirzaei: Mech. Syst. Signal Process. **168** (2022) 108593.
5 N. C. Minh, T. H. Dao, D. N. Tran, N. Q. Huy, N. T. Thu, and D. T. Tran: 2021 8th NAFOSTED Conf. Information and Computer Science (NICS) (IEEE, 2021) 33–38.
6 J. M. Chapa, K. Maschat, M. Iwersen, J. Baumgartner, and M. Drillich: Behav. Processes **181** (2020) 104262.
7 Y. S. Wu, W. Y. Wang, T. C. Chan, Y. L. Chiu, et al.: JMIR Serious Games **10** (2022) e35040.
8 A. Asadzadeh, T. Samad-Soltani, P. Rezaei-Hachesu, and Z. Salahzadeh: 2020 6th Int. Conf. Web Research (ICWR) (IEEE, 2020) 38–42.
9 P. Singh, P. Srivastava, R. K. Chaudhary, and P. Gupta: 2013 Int. Conf. Energy Efficient Technologies for Sustainability (IEEE, 2013) 896–900.
10 M. Benmessaoud and M. M. Nasreddine: Microsyst. Technol. **19** (2013) 713.